Radiative emission of driven two-level atoms into the modes of an enclosing optical cavity: The transition from fluorescence to lasing

A. Lezama,* Yifu Zhu, Manoj Kanskar, and T. W. Mossberg
Department of Physics, University of Oregon, Eugene, Oregon 97403
(Received 17 July 1989)

The radiative emission of strongly driven, two-level-like barium atoms into the modes of a confocal optical cavity is studied as a function of barium density. As the barium density is increased, the spatial profile, intensity, and spectrum of light emitted out the ends of the confocal cavity display dramatic changes indicative of a transition from fluorescence to lasing. In this novel two-level system, laser action can be explained in terms of an inversion between the dressed atom-field states or in terms of a type of stimulated hyper-Raman scattering in which atoms lase from the ground to the excited atomic state. A simple dressed-atom rate-equation analysis of this two-level-atom laser is presented. It is pointed out that this same system may provide a means of realizing two-photon-like laser action.

INTRODUCTION

Some time ago,[1–3] it was pointed out that population inversion (at least in the traditional sense) is not a prerequisite for optical gain in media consisting of strongly driven two-level atoms. Numerous theoretical works have subsequently elaborated on various aspects of this interesting result,[4–8] and experimental studies of the absorption spectrum of a weak probe beam interacting with an ensemble of strongly driven two-level atoms have indeed revealed regions of negative absorption or gain.[9,10] Just recently, Khitrova, Valley, and Gibbs,[11] working in a Doppler broadened sodium vapor, have demonstrated laser action based on this gain, and they point out that this gain relates to certain instabilities observed in driven systems. We note that a number of closely related effects involving amplification and gain via parametric interactions[12–16] and collisional effects[17,18] have also been found to occur in systems of driven two-level atoms, providing some additional measure of the richness of this fundamental system.

We present here the results of a study of driven two-level-atom gain performed in a simple Doppler-free system using nearly ideal two-level atoms. Specifically, we have studied the effect of gain on the radiative emission of driven two-level-like barium atoms into the degenerate modes of an enclosing confocal optical cavity.[8,19] In contrast to the case of Khitrova, Valley, and Gibbs,[11] our results are largely free of the complications associated with Doppler broadening, and they span regimes wherein the atomic emission is dominated by spontaneous as well as stimulated processes. In the former case, the cavity emission has the properties of strong-field resonance fluorescence,[20–23] while in the latter case, the atoms lase into the cavity modes. We attempt to characterize the transition from fluorescence to lasing in this elemental system by studying the spatial properties, spectral structure, and intensity of the cavity emission as a function of barium density.

It is interesting to note that the Mollow sideband gain observed in an ensemble of strongly driven two-level atoms can be explained from two very different perspectives. In one perspective, the presence of gain in this system can be portrayed as a result of the positive inversion that exists between certain pairs of dressed atom-field states when the driving-field frequency is detuned from the atomic transition frequency[4,24] (see Fig. 1). From another perspective, the gain arises from a two-photon Raman process (see Fig. 2), and the laser action can be viewed as a form of stimulated hyper-Raman scattering in which two pump photons are absorbed and the emission of one sideband photon is stimulated.[2] We will primarly adopt the former perspective, returning to the latter briefly when we discuss higher-order gain processes.

THEORY

We consider an ensemble of N_a two-level atoms of transition frequency ν_a located at the center of an open confocal optical cavity. The free-spectral range of the cavity is considered to be so large that only one cavity resonance interacts with the atoms. The atoms have a ground (excited) state $|g\rangle$ ($|e\rangle$) [see Fig. 1(a)]. The atoms are driven by a strong, coherent-state, pump field of frequency ν_l, detuning $\Delta \equiv \nu_l - \nu_a$, and resonance Rabi frequency Ω_0. The pump propagates transverse to the cavity axis. The pump-field energy spectrum consists of a ladder of number states $|n\rangle$, as shown in Fig. 1(b). On coupling the atoms and the pump field, we obtain the well-known dressed states $|i,n\rangle$ $(i=1,2)$ of the pump plus atom system.[4,25] The dressed energy spectrum consists of a ladder of doublets separated by ν_l and split by $\nu_s \equiv (\Delta^2+\Omega_0^2)^{1/2}$ [see Fig. 1(c)]. The asymptotic decomposition of the dressed states in terms of atom-pump product states for large positive and negative Δ is also shown. Let Π_i be the population of the dressed-state component i $(i=1,2)$ summed over n. We assume that A_{ij} is the total spontaneous-emission rate from the ith to the jth dressed-state components in adjacent doublets,

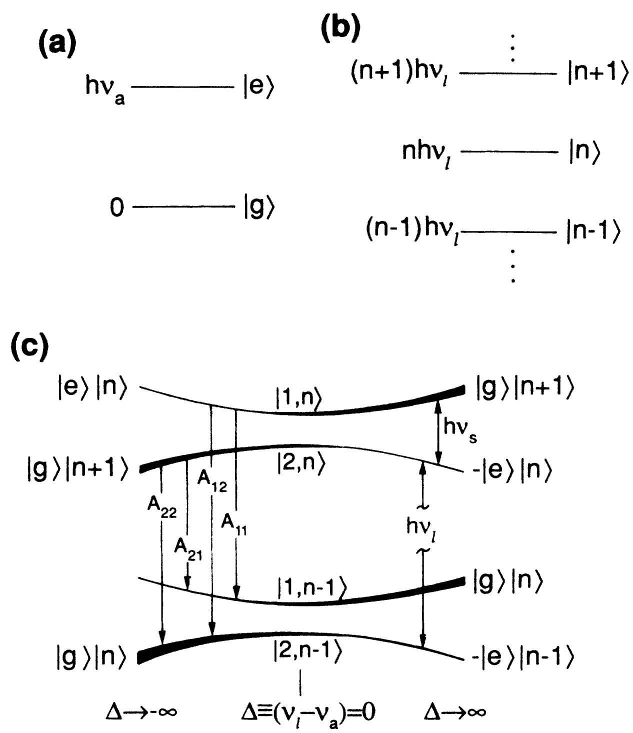

FIG. 1. Schematic energy diagram of (a) the two-level atom, (b) the quantized pump field, and (c) the dressed atom, i.e., the coupled atom-field system. In (c), the atom-field product states at the right (left) represent the asymptotic dressed-state composition for large positive (negative) detuning Δ. The thickness of the lines representing the energy levels in (c) provides a qualitative indication of the relative population of the corresponding level.

and that a_{ij} is the corresponding spontaneous-emission rate into the cavity modes. Let n_c be the mean number of photons in the cavity having the cavity resonance frequency, and let $B_{ij}n_c$ be the rate of stimulated transitions from the ith to the jth dressed-state component of adjacent doublets induced by the cavity-mode field. In the case of a simple single-mode cavity, a_{ij} and B_{ij} have the same magnitude. In a highly degenerate cavity, like the

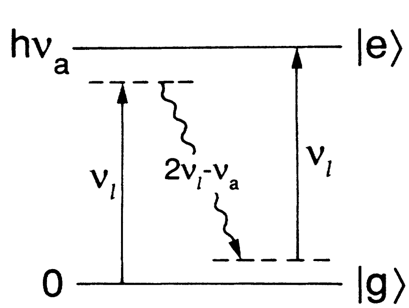

FIG. 2. Stimulated Raman process to which the driven two-level-atom gain of interest here can be attributed (Ref. 2). Note that this process transfers population from the ground to the excited state.

one we consider, the situation is more complex, and we retain these two quantities distinct throughout our calculation.

Considering, for example, the case of $\Delta < 0$, the $|2,n\rangle$ dressed-state components take on more of the character of the atomic ground state, and can thus be expected to be more heavily populated under steady-state conditions than the $|1,n\rangle$ dressed-state components. Consequently, an inversion on dressed-state transitions of the form $|2,n\rangle \rightarrow |1,n-1\rangle$ will exist and provide for gain at the corresponding transition frequency. By similar arguments, one can predict the existence of absorption at the frequency of the $|2,n-1\rangle \rightarrow |1,n\rangle$ transitions.

One can immediately write down rate equations governing the populations of the dressed states, the mean number of photons in the cavity, and therefore of the intensity of light emitted out the ends of the cavity. For $\Delta < 0$ and with the cavity resonant with the inverted transition, we have

$$\dot{\Pi}_2 = \Pi_1(A_{12} + B_{21}n_c) - \Pi_2(A_{21} + B_{21}n_c) \,, \tag{1a}$$

$$\dot{n}_c = -kn_c + B_{21}n_c(\Pi_2 - \Pi_1) + a_{21}\Pi_2 \,, \tag{1b}$$

and

$$\Pi_1 + \Pi_2 = N_a \,, \tag{1c}$$

where k is the cavity loss rate. Setting the derivatives to zero and solving for n_c, one obtains

$$n_c = \frac{q \pm (q^2 + 8kB_{21}a_{21}A_{12}N_a)^{1/2}}{-4kB_{21}} \,, \tag{2a}$$

where

$$q = k(A_{21} + A_{12}) - B_{21}N_a[A_{12} - (A_{21} - a_{21})] \,. \tag{2b}$$

In the limits of small and large N_a, n_c has a simple linear dependence on the number of atoms present, i.e., for N_a small

$$n_c = \frac{A_{12}a_{21}N_a}{k(A_{21} + A_{12})} \,, \tag{3a}$$

and for N_a large

$$n_c = \frac{[A_{12} - (A_{21} - a_{21})]N_a}{2k} \,. \tag{3b}$$

For small N_a, the growth in n_c is determined by spontaneous emission into the cavity mode. For higher N_a, stimulated processes dominate and n_c becomes limited by the pumping rate. In the present system, pumping can be viewed as spontaneous emission on transitions of the form $|1,n\rangle \rightarrow |2,n-1\rangle$, and it proceeds at the rate A_{12}. The laser threshold corresponds to the slope change observed on passing from Eq. (3a) to Eq. (3b).

In distinction to more standard laser systems in which the spontaneous-emission rates are constants, in the two-level-atom laser A_{21} and A_{12} are functions of Δ and the resonant pump-field Rabi frequency Ω_0. We have

$$A_{12} = \alpha_{12}\rho_{12}\cos^4(\theta) \tag{4a}$$

and

$$A_{21}=\alpha_{21}\rho_{21}\sin^4(\theta) , \tag{4b}$$

where $\alpha_{ij}=(\pi\nu_{ij}/3\epsilon_0\hbar)|p|^2$, ν_{ij} is the relevant dressed-state transition frequency, $|p|$ is the appropriate transition matrix element connecting the atomic ground and excited states, and ρ_{ij} is the density of electromagnetic modes per unit volume and frequency at the frequency of the corresponding dressed-state transition. Also

$$2\theta=\tan^{-1}(-\Omega_0/\Delta) . \tag{4c}$$

In the high-N_a limit, Eqs. (1) can be analyzed to show that the populations of the dressed-state components become equalized (i.e., $\Pi_1=\Pi_2$), implying the same for the bare-state ($|g\rangle,|e\rangle$) populations. In the limit of small N_a, on the other hand, the dressed-state component with the largest admixture of the atomic ground state is preferentially populated. This result indicates that the onset of lasing results in a net transfer of population from the ground to the excited atomic state. In other words, the atoms lase upwards in energy. This rather novel result is consistent with the perspective that the lasing observed in the driven two-level-atom system can be viewed as a form of stimulated hyper-Raman scattering.[2] Note, however, that in the present case, the population transfer does not involve a virtual transition through a third level.

APPARATUS

In our experiments, a thermal, 1-mm-diam atomic beam of natural Ba was made to pass through the center of a 1-cm-long symmetric confocal cavity. Cavity mirrors were 5 mm in diameter, but one of them was limited to a 300-μm clear aperture. Measured cavity finesse was about 200. The cavity spacing and hence its resonance frequency was tuned by using a piezoelectric transducer attached to one of the mirrors. A collimated, 2-mm-diam beam from a single-mode cw ring laser intercepted the atomic beam at the geometrical center of the cavity. The atomic beam, pump beam, and cavity axis were made mutually orthogonal to provide for nearly Doppler-free observations and to suppress nonlinear effects dependent on phase matching. The laser was linearly polarized with its electric field vector perpendicular to the cavity axis, and was tuned near to resonance with the 553.5-nm $6s^2\,{}^1S_0\rightarrow 6s6p\,{}^1P_1$ ^{138}Ba transition. The compensated ambient magnetic field in the interaction region was <1 G. The laser frequency was actively locked to a magnetically tunable saturation resonance in an auxiliary Ba vapor cell. The fluorescent light emitted out one side of the cavity was recorded to provide a relative measure N of the total number of atoms present in the interaction region as the temperature of the atomic source was varied. The light emitted out one end of the cavity (axial emission) was spatially filtered and detected. We refer to measurements of the axial emission as a function of cavity resonance frequency as the axial emission spectrum.

In a previous publication,[19] we reported measurements of the axial emission spectrum for Ba beam densities below those required for lasing. At very low Ba densities, the axial emission spectrum duplicates the well-known symmetric Mollow triplet familar from strong-field resonance fluorescence work.[20–23] At higher densities, the spectrum was found to become asymmetric, one sideband was strongly enhanced while the other was suppressed. The enhanced sideband corresponds to the inverted dressed-state transition. In the present experiment, modifications to the atomic beam source have enabled us to reach Ba densities high enough to support lasing. At the maximum Ba beam density employed, the weak signal absorption at the center of the ^{138}Ba resonance line was measured to be approximately 30%. We used an on-resonance pump Rabi frequency of $\Omega_0\simeq 230$ MHz, and fixed the laser-atom detuning at $\Delta=-100$ MHz. Here $\Delta<0$ was chosen to minimize the influence of the other Ba isotopes, all of which have transition frequencies above that of ^{138}Ba.

EXPERIMENTAL OBSERVATIONS

In Fig. 3, we present measurements of the axial emission intensity as a function of barium beam density with the cavity tuned to the frequency of the degenerate $1\rightarrow 1$ and $2\rightarrow 2$ dressed-state transitions (trace *a*) and to the frequency of the inverted $2\rightarrow 1$ dressed-state transition (trace *b*). The variation in emitted intensity versus density observed in the two cases is strikingly different. With the cavity tuned to the central Mollow peak ($1\rightarrow 1$ and $2\rightarrow 2$ transitions), the output intensity exhibits a slightly sublinear variation with Ba density, which, as discussed in Ref. 19, is attributable to absorption arising from weakly driven atoms located near the edges of the pump laser beam. The steplike structure seen in trace *b* of Fig. 3, corresponds to the slope change expected to occur [see Eq. (3)] with the onset of lasing on the inverted $2\rightarrow 1$ dressed-state transition.

In Fig. 4, the axial output intensity as a function of cavity tuning is shown for two different Ba beam densities. In each part of the figure, the relative atomic density is given in the same units as employed in Fig. 3. Fig-

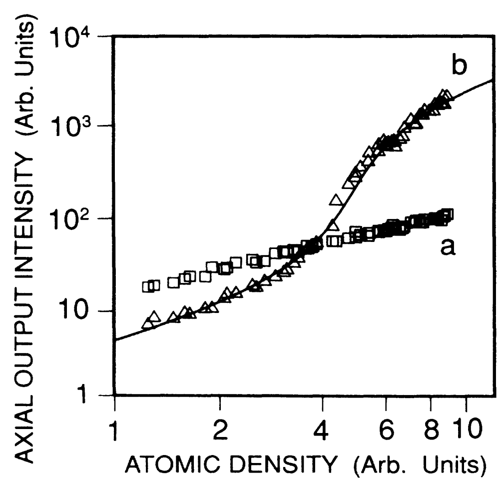

FIG. 3. Measured intensity of axial emission vs relative atomic density for $\Delta=-100$ MHz and $\Omega_0=230$ MHz with the cavity tuned to (a) the central Mollow peak and (b) the sideband exhibiting gain. The solid line is a fit of the data to Eq. (2a) (see text).

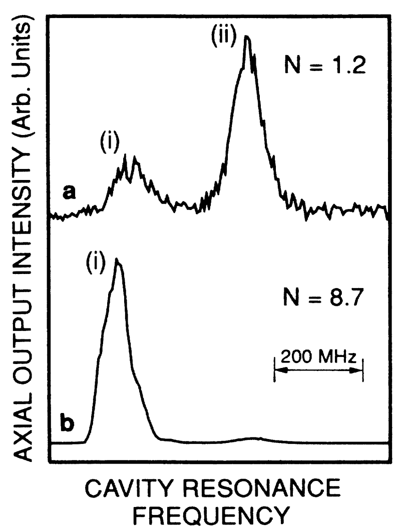

FIG. 4. Measured axial emission intensity vs cavity resonance frequency (horizontal) for two different relative Ba densities. (i) corresponds to the inverted $|2,n\rangle$-$|1,n-1\rangle$ type transitions, while peak (ii) corresponds to the central Mollow peak. The high-frequency sideband is totally suppressed due to absorption. The relative atomic density in the units of Fig. 3 is indicated for each case. The horizontal scale has a full range of 0.8 GHz.

ure 4(a) was recorded below the laser threshold, but the spectrum is significantly altered from the classic Mollow form,[20] which consists of a central peak at frequency ν_l and two sidebands at the frequencies $\nu_l \pm \nu_s$. In the present case, the peak (i), corresponding to the inverted $2 \rightarrow 1$ dressed-state transition at frequency $\nu_l - \nu_s$, is amplified while the opposite sideband, corresponding to the uninverted and hence absorptive $1 \rightarrow 2$ dressed-state transition at frequency $\nu_l + \nu_s$, is so highly attenuated that it cannot be seen. Peak (ii) at frequency ν_l corresponds to the central component of the Mollow triplet. Figure 4(b) was recorded at a barium density above the laser threshold. Notice that the amplified sideband now dwarfs the central peak.

Finally, with the cavity tuning fixed, we have measured the spectrum (Fig. 5) and the spatial profile (Fig. 6) of the light emitted axially out of the cavity for various cavity resonance frequencies ν_c and a constant large barium density. Output spectra were measured using an external 50-cm, 5-MHz resolution, 150-MHz free-spectral range, confocal Fabry-Pérot spectrum analyzer. In recording

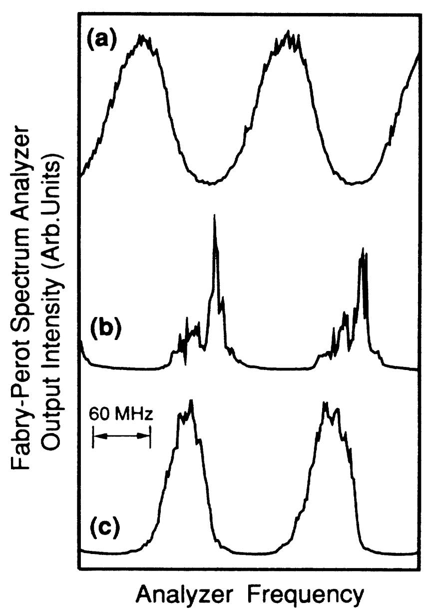

FIG. 5. Frequency spectrum of the axial light output for different cavity tunings. (a) Cavity tuned to the central Mollow peak, (b) cavity slightly detuned from the inverted dressed-state transition frequency ($\nu_l - \nu_s$) (see Fig. 1), (c) cavity tuned to the maximum of the gain profile for the enhanced sideband. In obtaining the spectra shown here, the Fabry-Pérot analyzer was scanned over slightly more than two 150-MHz free-spectral ranges.

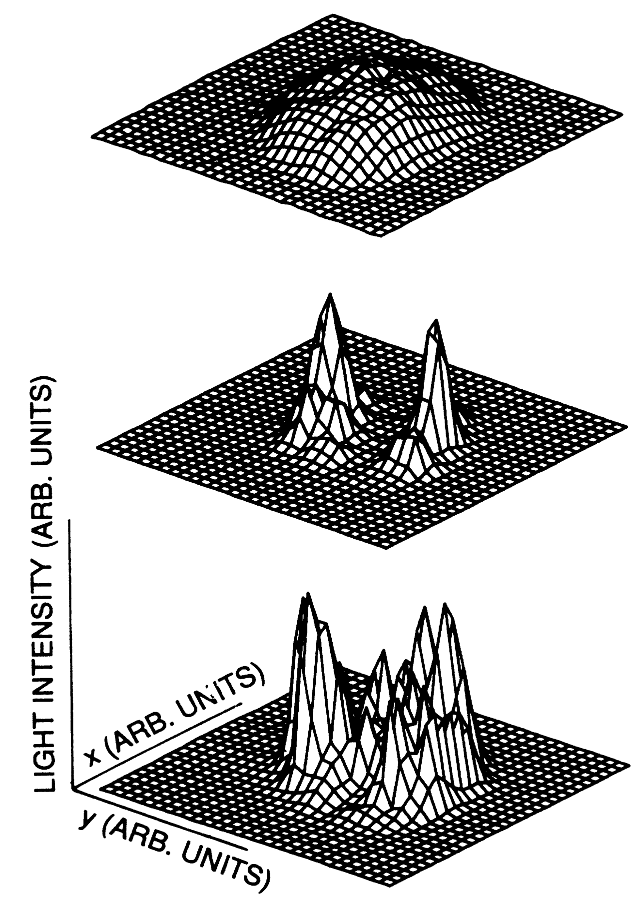

FIG. 6. Spatial light intensity profile at the optical image of the center of the cavity. The vertical axis is proportional to the intensity of the light and the transverse axes to spatial position. Each part of this figure was recorded under the same conditions as the corresponding part of Fig. 5.

the spectra of Fig. 5, the 50-cm Fabry-Pérot analyzer was scanned through approximately two free-spectral ranges producing two recordings of each spectrum separated horizontally by the 150-MHz free-spectral range of the Fabry-Pérot analyzer. For these measurements, the Ba beam density was $\simeq 9$ in the relative density units of Fig. 3. In Fig. 5(a), the cavity is tuned to the central peak of the resonance fluorescence spectrum at frequency ν_l. In Fig. 5(b), the cavity is tuned near the $2 \rightarrow 1$ transition frequency $(\nu_l - \nu_s)$ slightly off from the maximum gain position. In Fig. 5(c), the cavity is tuned near the $2 \rightarrow 1$ dressed-state transition frequency so as to optimize the cavity output intensity. The spatial axial-output-intensity distributions shown in Fig. 6 were recorded by imaging the center of the cavity onto a CCD array detector. The corresponding parts of Figs. 5 and 6 were recorded simultaneously.

ANALYSIS

The results presented above characterize and are consistent with a transition from spontaneous to stimulated atomic emission into the cavity modes. The magnitude of the step shown in Fig. 3 is determined [see Eq. (3)] by the ratio of A_{21}/a_{21}. In the present case, the observed step size is small, but this is entirely consistent with the small value of the ratio A_{21}/a_{21} characteristic of our small mode-degenerate optical cavity. Using the measured values of Ω_0, Δ (to determine A_{21} and A_{12}), and k, we have adjusted the value of the ratio a_{21}/A_{21} in Eq. (2) to fit the step size (slope change) experimentally observed (Fig. 3, trace *b*). The best fit is obtained for $a_{21}/A_{21} \simeq 2 \times 10^{-2}$. The corresponding calculated variation of n_c with N_a is shown in Fig. 3 as the solid line. The value obtained for a_{21}/A_{21} is in good agreement with the experimentally measured value of 0.05 obtained under similar experimental conditions in the same cavity.[24] We note that the ratio B_{ij}/a_{ij} determines the horizontal location of the step (laser transition) in Fig. 3, but does not affect the step size. This ratio was adjusted to achieve horizontal overlap of the experimental and theoretical curves.

The results shown in Figs. 5 and 6 demonstrate the dramatic changes in the spectral and spatial structure of the axial cavity emission that coincides with the onset of lasing. In Fig. 5(a), which shows the spectrum of the cavity output when the cavity is tuned to the central peak of the Mollow triplet, the observed linewidth (60 MHz) is due to the natural linewidth of the transition and to residual Doppler width. No structure is observed in the line. Similar results were obtained with the cavity tuned to either of the Mollow sidebands at very low atomic density, where the atomic radiation is due to spontaneous emission. The spatial profile of the cavity output obtained under the conditions just discussed [Fig. 6(a)] is smooth and featureless. This observation is entirely in agreement with the spatial profile expected in the case of fluorescence from an extended atomic sample. Under lasing conditions (large N and the cavity tuned to the enhanced Mollow sideband) a very different behavior is observed. With the cavity slightly detuned from the inverted dressed-state transition (corresponding to reduced gain), very sharp structures appear both in the spectral [Fig. 5(b)] and in the spatial [Fig. 6(b)] profile of the cavity field. The individual peaks in the output spectrum have widths determined by the resolution of the Fabry-Pérot analyzer (5 MHz). These peaks are substantially narrower than the free-space natural atomic linewidth (19 MHz). At the same time the spatial profile of the field becomes nonuniform. Both results can be understood by assuming that the gain in the medium is just enough to bring a few of the cavity modes above the lasing threshold. These modes would be the ones most efficiently coupled to the atomic medium. The peaks observed in the spectrum correspond to the small number of modes above threshold. The spectral narrowness of the peaks [Fig. 5(b)] results from an increase in the field correlation time associated with the laser oscillation. The spatial intensity pattern observed corresponds to the field distribution of the lasing modes. It is important to point out that the results shown in Figs. 5(b) and 6(b) correspond to a particular observation. Minor changes in the experimental parameters result in a large variety of spectral and spatial patterns with similar qualitative characteristics. As the cavity is tuned to the maximum gain frequency [Figs. 5(c) and 6(c)], the number of lasing modes is increased. It is no longer possible to resolve the frequencies of the individual modes and the spatial pattern becomes increasingly complicated.

TWO-PHOTON TWO-LEVEL-ATOM LASER

As mentioned earlier, the gain discussed in this paper can be attributed to the Raman-type process shown in Fig. 2. In Fig. 7, we show a higher-order Raman process in which three pump photons are absorbed, two photons are emitted, and the atoms are promoted to the excited state. In a cavity, the frequencies of the emitted photons can be constrained to be equal, and we have what amounts to a two-photon gain process. Since the process is nearly resonant at every step, the associated two-photon gain, which in the weak-field limit arises at the frequency $\nu_l + (\nu_l - \nu_a)/2$, should be relatively strong and provide a means of realizing an optical two-photon laser. A dressed-state analysis of this possibility will be published elsewhere.

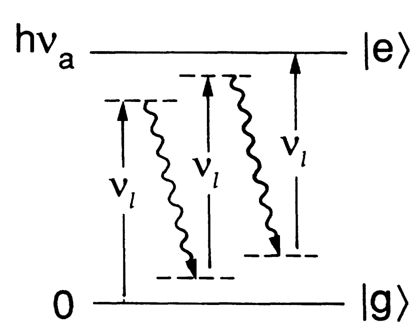

FIG. 7. Possible mechanism for two-photon gain in systems of driven two-level atoms.

CONCLUSIONS

We have experimentally demonstrated that laser action can take place in very simple system, i.e., a nearly homogeneous ensemble of strongly driven two-level atoms. The dynamics of this novel laser is entirely determined by radiative processes with dressed-atom spontaneous emission serving as both a pumping and a damping mechanism. Interestingly, in this system, the lasing takes place in the absence of atomic inversion and results in the increase of the excited-state population. The two-level-atom laser constitutes the realization of a new regime of driven-atom dynamics where the usual relaxation through spontaneous emission is replaced by an alternate sequence of spontaneous and stimulated emission processes. Although the simple rate-equation treatment of the system accounts for the features studied here, a more detailed theoretical analysis of this new dynamical regime is necessary. Finally, we point out that the driven two-level-atom system may provide a means of achieving steady-state optical two-photon gain.

ACKNOWLEDGMENTS

It is a pleasure to thank Professor M. G. Raymer for lending us a Video Frame Grabber and many useful discussions. We thank expert assistance of S. J. Kuo and S. E. Hodges. This work is supported by the National Science Foundation (Grant No. PHY-8718518) and Air Force Office of Scientific Research (Grant No. AFOSR-88-0086). One of us (A.L.) acknowledges support from the Conselho Nacional de Desenvolvimento Cientifico e Tecnologico (Brazil).

---

*Present address: Departamento de Fisica, Pontificia Universidade Catolica de Rio de Janeiro, Caixa Postal 38071, 22452 Rio de Janeiro, Brazil.

[1]B. R. Mollow, Phys. Rev. A **5**, 2217 (1972).

[2]S. Haroche and F. Hartmann, Phys. Rev. A **6**, 1280 (1972).

[3]S. L. McCall, Phys. Rev. A **9**, 1515 (1974).

[4]C. Cohen-Tannoudji and S. Reynaud, J. Phys. B **10**, 345 (1977).

[5]G. Khitrova, P. R. Berman, and M. Sargent III, J. Opt. Soc. Am. B **5**, 160 (1988).

[6]G. S. Agarwal, Phys. Rev. A **19**, 923 (1979).

[7]R. W. Boyd and M. Sargent III, J. Opt Soc. Am. B **5**, 99 (1988).

[8]D. A. Holm, M. Sargent III, and S. Stenholm, J. Opt. Soc. Am. B **2**, 1457 (1985).

[9]F. Y. Wu, S. Ezekiel, M. Ducloy, and B. R. Mollow, Phys. Rev. Lett. **38**, 1077 (1977).

[10]M. T. Gruneisen, K. R. MacDonald, and R. W. Boyd, J. Opt. Soc. Am. **5**, 123 (1988).

[11]G. Khitrova, J. F. Valley, and H. M. Gibbs, Phys. Rev. Lett. **60**, 1126 (1988).

[12]A. C. Tam, Phys. Rev. **19**, 1971 (1979).

[13]D. J. Harter, P. Narum, M. G. Raymer, and R. W. Boyd, Phys. Rev. Lett. **46**, 1192 (1981).

[14]R. W. Boyd, M. G. Raymer, P. Narum, and D. J. Harter, Phys. Rev. A **24**, 411 (1981).

[15]D. J. Harter and R. W. Boyd, Phys. Rev. A **29**, 739 (1984).

[16]D. Grandclement, G. Grynberg, and M. Pinard, Phys. Rev. Lett. **59**, 44 (1987).

[17]G. Grynberg, E. LeBihan, and M. Pinard, J. Phys. (Paris) **47**, 1321 (1986).

[18]D. Grandclement, G. Grynberg, and M. Pinard, Phys. Rev. Lett. **59**, 40 (1989).

[19]Y. Zhu, A. Lezama, and T. W. Mossberg, Phys. Rev. A **39**, 2268 (1989).

[20]B. R. Mollow, Phys. Rev. **188**, 1969 (1969).

[21]W. Hartig, W. Rasmussen, R. Schieder, and H. Walther, Z. Phys. A **278**, 205 (1976).

[22]F. Schuda, C. R. Stroud, Jr., and M. Hercher, J. Phys. B **7** L198 (1974).

[23]R. E. Grove, F. Y. Wu, and S. Ezekiel, Phys. Rev. A **15**, 227 (1977).

[24]As recently demonstrated, dressed-state inversions can be controlled by introducing spectral structure into the electromagnetic vacuum and dressed-state inversions can be created even when the atom and driving field are exactly resonant. See Y. Zhu, A. Lezama, T. W. Mossberg, and M. Lewenstein, Phys. Rev. Lett. **61**, 1946 (1988); A. Lezama, Y. Zhu, S. Morin, and T. W. Mossberg, Phys. Rev. A **39**, 2754 (1989). For related results see M. Lindberg and C. M. Savage, Phys. Rev. A **38**, 5182 (1988). In the present experiment, the mode-degenerate cavity employed introduces a small ($\simeq 5\%$) variation in the electromagnetic mode density across the Mollow triplet. This variation is not expected to play a major role in our experiments and is ignored in the analysis.

[25]C. Cohen-Tannoudji, in *Frontiers in Laser Spectroscopy,* Proceedings of the Les Houches Lectures, Session XXVII, 1975, edited by R. Balian, S. Haroche, and S. Liberman (North-Holland, New York, 1977).